

## The Influence of Plastic Deformation on the Structure of Passive Films on Carbon Steel in Simulated Pore Solution

Xingguo Feng,<sup>a</sup> Xiangyu Lu,<sup>b</sup> Yu Zuo<sup>b</sup> and Da Chen<sup>\*a</sup>

<sup>a</sup>Key Laboratory of Coastal Hazards and Protection of the Ministry of Education, College of Harbour, Coastal and Offshore Engineering, Hohai University, Nanjing 210098, Jiangsu, China

<sup>b</sup>School of Materials Science and Engineering, Beijing University of Chemical Technology, Beijing 100029, China

O processo de passivação de aço carbono durante deformação plástica em uma solução simulada de poro foi estudado usando-se testes eletroquímicos e microscopia de força atômica (AFM). Os resultados de polarização mostram que a atividade do aço carbono aumentou com o aumento do grau de deformação. Antes da ruptura dos filmes passivos, as amostras altamente deformadas apresentaram um alto potencial de circuito aberto (OCP). Por outro lado, o tempo de incubação de pite diminuiu com o aumento da deformação plástica. Os resultados de Mott-Schottky sugerem que a grande deformação tornou altamente dopados os filmes passivos. Além disso, as camadas de cargas espaciais dos filmes passivos afinaram quando a deformação plástica aumentou. As observações por AFM indicaram que os filmes passivos se tornariam menos homogêneos com aumento da deformação. Estes resultados demonstram que filmes passivos em aço carbono deformado se tornam instáveis quando a deformação plástica aumenta.

The process of passivation of carbon steel when experiencing plastic deformation in simulated pore solution has been studied using electrochemical tests and atomic force microscopy (AFM). The polarization results show that the activity of the carbon steel increased with increasing degree of deformation. Before the passive films were ruptured, the heavily deformed samples presented a high open circuit potential (OCP). On the other hand, the pitting incubation time decreased with increasing plastic deformation. The Mott-Schottky results suggested that the high deformation caused the passive films to be heavily doped. In addition, the space charge layers of passive films were thinned when the plastic deformation increased. The AFM observations indicated that the passive films become more inhomogeneous as the deformation increased. These results demonstrate that passive films on the deformed carbon steel become unstable when the plastic deformation increases.

**Keywords:** concrete, carbon steel, passive films, Mott-Schottky, AFM

### Introduction

Under normal conditions, the high alkalinity of concrete promotes the formation of a stable passive film on the steel bar, protecting it from corrosion. Environmental factors, such as chloride concentration, temperature and stress, also exert important effects on the passive behavior of rebars. In particular, engineering concrete structures are always subjected to a number of stresses. Thus, clarifying the passive behavior and corrosion characteristics of rebars under stress is important for conservation and restoration

of concrete structures. Schroeder *et al.*<sup>1</sup> studied the stress corrosion cracking (SCC) of AISI 1080 steel in simulated concrete pore solution and concluded that the action of hydrogen was closely related to the fracture mechanism of SCC. Vu *et al.*<sup>2</sup> found that local defects on the steel surface lead to an increase of SCC for the stress concentration. Moreover, the authors<sup>2</sup> also noticed that the service life of rebars obviously decreased as the stress level increased. Consequently, as earlier research,<sup>1,2</sup> stresses significantly affect the durability of concrete structures.

To investigate the effects of stress on the initial stage of SCC, some authors<sup>3-8</sup> studied the passive behavior of metals under various types of stress. In a borate buffer

\*e-mail: chenda@hhu.edu.cn

solution containing chloride, with a pH of 8.45, Yang *et al.*<sup>3</sup> investigated the passive behavior of 304 stainless steel under tensile stress. The results showed that the critical chloride concentration, which was related to the rupture of passive films, decreased as the tensile stress increased. Díaz *et al.*<sup>4</sup> studied the depassivation behavior of high strength steels under tensile stress in cement extract using electrochemical tests. They concluded that the passive films would be irreversibly damaged even in a solution containing a low concentration of chloride ( $0.01 \text{ mol L}^{-1}$ ). Vignal *et al.*<sup>5,6</sup> investigated the semi-conducting behavior of passive films on 316L stainless steel under elastic stress. Their results suggested that high elastic stress caused the passive films to be heavily doped. In addition, the heavily doped films were sensitive to pitting corrosion. In another report, Zhang *et al.*<sup>7</sup> studied the passive behavior of pre-cracked X70 pipeline steel in carbonate/bicarbonate solution under tensile stress. The authors proposed that both the crack-tip and the region ahead of the cracks could be passivated. However, their results also indicated that the passive films at the crack tip were less stable and susceptible to pitting corrosion. Studying the micro-electrochemical behavior of duplex stainless steel in several aqueous electrolytes, Vignal *et al.*<sup>8</sup> concluded that the corrosion potential of substrate increased linearly with the local residual compressive stress. In a  $\text{K}_2\text{SO}_4$  solution containing  $10 \text{ mmol L}^{-1} \text{ K}_3\text{Fe}(\text{CN})_6$ , Sidane *et al.*<sup>9</sup> researched the passive behavior of 304 stainless steel under static tensile stress. Scanning electrochemical microscope (SECM) results indicated that the kinetic constant of the mediator oxidation on the substrate increased significantly with the stress magnitude. Zhu *et al.*<sup>10</sup> studied the activity of Alloy 800 under stress and found that both tensile stress and compression stress enhanced the activity of the surface.

Previous research has focused mainly on the negative effects<sup>3,5-7</sup> of stress on passive films in acid or neutral solution. However, there is very little research<sup>4</sup> into the effects of stress on passive behavior in alkaline solutions. In the present study, the influence of plastic deformation on the structure of passive films for carbon steel was studied in cement extract. The results suggest that passive films will be heavily doped when the carbon steels are subjected to high deformation. In addition, the thickness of the space charge layer decreased with increasing deformation magnitude. The uniformity of the passive films also decreased with the degree of deformation.

**Table 1.** The ion concentrations of the cement extracts

Ion	$\text{K}^+$	$\text{Ca}^{2+}$	$\text{Na}^+$	$\text{SO}_4^{2-}$	$\text{Cl}^-$
Concentration / ( $\text{mol L}^{-1}$ )	$5.53 \times 10^{-5}$	$2.63 \times 10^{-5}$	$9.79 \times 10^{-5}$	$2.13 \times 10^{-5}$	$7.43 \times 10^{-6}$

## Experimental

### Materials and solution

The carbon steel samples used in this study were  $160 \text{ mm} \times 15 \text{ mm} \times 1 \text{ mm}$ . The chemical composition of the steel was (wt.%): 0.37% C, 0.16% Si, 0.32% Mn, 0.053% S, 0.026% P and Fe. The samples for the electrochemical tests were ground with emery papers up to No. 600, while these for AFM observation were further ground to No. 2000 and then polished with diamond paste ( $1 \mu\text{m}$ ). Afterwards, the samples were degreased with acetone. Leaving an exposed area with a size of  $1 \text{ cm} \times 1 \text{ cm}$  in the middle, the other areas of the samples were covered with a coating of TALLY 8516G silica-gel (one component, room temperature curing silica-gel, produced by TALLY Chemical Industrial Co., Ltd., Chendu, China), as shown in Figure 1. For the carbon steel studied, plastic deformation occurred when the strain was above 0.62%.

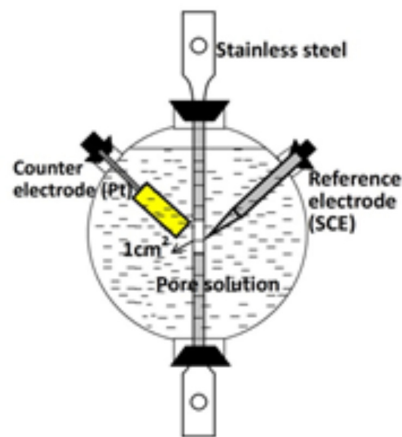


**Figure 1.** Illustration of the sample and the model used for electrochemical tests.

The cement extract (CE) solution was prepared by adding 500 g blend Portland cement to 1 L deionized water.<sup>4,11,12</sup> The liquid was stirred for 15 min and kept for 30 min, then filtered. The filtered liquid, with a pH of 12.74, was used as the pore solution. The cations of the cement extract were analyzed with an ICP-MS7500CE (Agilent, USA) inductively coupled plasma mass spectrometer, and the anions were tested with an ICS3000 (DIONEX, USA) ion chromatography system. The concentrations of different ions for the cement extract are presented in Table 1.

## Measurement techniques

Using a 100 mm initial distance between marks, different plastic deformations, including 0.77%, 2.65%, 3.87%, 7.14%, were chosen for studying the effects of plastic deformation on the passive behavior of carbon steel. For comparison, the passivation behavior of the control samples (without deformation) was also investigated. The deformations of samples were conducted using a universal testing machine (LETRY Machine Company, Xi'an, China) at a strain rate of  $1 \text{ mm min}^{-1}$  until reaching the designed strain.

All electrochemical tests were performed with a CS350 electrochemical workstation (Corrtest Instrument, China). With a platinum plate as the counter-electrode and a saturated calomel electrode (SCE) as the reference electrode, the classical three electrodes were used in the electrochemical measurements. The reference electrode was kept as close as possible to the working electrode. Each experiment was replicated three times and a new sample was used every time. To reduce the air-formed oxide film, all samples were cathodically polarized at a potential of  $-0.6 \text{ V}$  for  $5 \text{ min}^{13}$  before testing. The anodic polarization curves were conducted at the rate of  $1 \text{ mV s}^{-1}$  after the samples were stabilized for 1 h in the pore solution. To study the stability of passive films, the current fluctuations of samples in the potentiostat when polarized at  $0.4 \text{ V}^{3,14}$  were recorded. In addition, the OCP was recorded until the breakdown of the passive film. Furthermore, capacitance measurements and Mott-Schottky analyses were performed to study the semiconducting properties of the passive films. After 2 h of passivation in the pore solution, capacitance measurements were carried out potentiostatically in potential steps of  $50 \text{ mV}$  from  $-1.0$  to  $1.0 \text{ V}$ . Using a  $10 \text{ mV}$  superimposed AC signal, scans were performed at a frequency of  $1000 \text{ Hz}^{15-17}$ .

To study the influences of plastic deformation on the morphology of passive films, after 24 h of passivation in pore solution at OCP, the films on the polished carbon steel were investigated by a Solver P-47H (NT-MDT Company, Russia) multimode AFM instrument. With a  $0.6 \text{ N m}^{-1}$  spring constant for the cantilever, images were taken in a non-contact mode using a  $\text{Si}_3\text{N}_4$  tip. The AFM topographic images were recorded over  $500 \text{ nm} \times 500 \text{ nm}$  scan areas, with a resolution of  $256 \times 256$  data points.

## Results and Discussion

### Polarization results

Anodic polarization curves for the different deformation samples were measured after 1 h of stabilization in the pore

solution at OCP. As the deformation increased, the OCP of the samples are  $-0.248$ ,  $-0.244$ ,  $-0.234$ ,  $-0.226$  and  $-0.232 \text{ V}$ , respectively. This result suggests that the OCP slightly increased with increasing deformation magnitude. Meanwhile, as Figure 2 shows, the anodic current density increased as the plastic deformation increased. The anodic polarization results indicated that the activity of substrate increased with increasing magnitude of deformation.

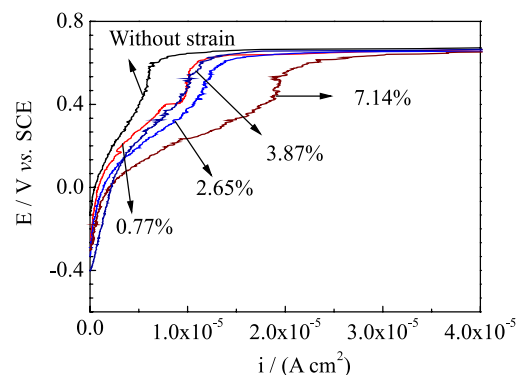


**Figure 2.** The anodic polarization curves for different strains after 1 h of passivation in pore solution.

According to the results shown in Figure 2,  $0.4 \text{ V}$  is in a passive-active transition state for the carbon steel in the cement extract. In the transition potential, a sudden increase of current density is related to the rupture of passive films.<sup>14</sup> Thus, the samples were polarized at  $0.4 \text{ V}$  to study the stability of the passive films. As Figure 3 shows, the fluctuation of current densities became frequent as the plastic deformation increased. Therefore, the current density transient results indicate that the stability of passive films decreased with increasing degree of deformation. On the other hand, the current density increased significantly with plastic deformation. This situation is consistent with the anodic polarization results (Figure 2); the activity of the carbon steel increases with the degree of deformation.

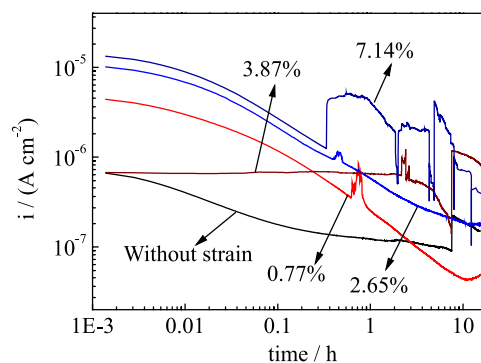


**Figure 3.** Plots of current vs. time of the samples subjected to different strains during potentiostatic polarization at  $0.4 \text{ V}$  in the cement extract solution.

## OCP results

The evolutions of OCPs for samples with different degree of deformation in the cement extract are presented in Figure 4. As the results show, the OCP of carbon steel increases as the passivation progresses. However, after a certain time, the OCP decreases suddenly and then visible pitting corrosion is observed over the exposed area. Vignal *et al.*<sup>5</sup> reported that the adsorption of chloride was enhanced by tensile stress. As exposure continues, the concentration of chloride in some regions of the film/solution interface can reach a critical value, and then the passive films crack at those regions. In addition, as shown in Figure 5, before the passive films breakdown, the OCPs of samples in the cement extract increased with increasing plastic deformation. Furthermore, the pitting incubation time (the time before a sudden drop of OCP) of carbon steel decreases significantly with increasing plastic deformation (Figure 6). Therefore, passive films became unstable as the plastic deformation increases in the cement extract.

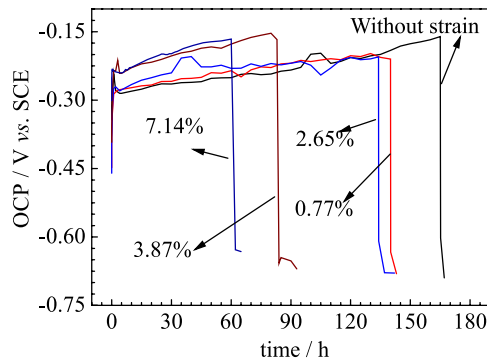


**Figure 4.** OCP results for samples with different degree of deformation during passivation in the cement extract.

## Semiconducting properties of passive films under plastic deformation

The capacitance-potential curves of different plastic deformation samples are presented in Figure 7. Along with typical capacitance behavior of metals with passive films,<sup>15,18</sup> the capacitance of the passive films on deformed carbon steel is about  $5 \mu\text{F cm}^{-2}$ . When the potential is below  $-0.5 \text{ V}$ , the capacitance decreases with increasing potential. Dong *et al.*<sup>16</sup> proposed that the decrease in capacitance is ascribed to a depletion layer of donors on the passive film/electrolyte interface. As the potential is in the range  $-0.5$  to  $0.5 \text{ V}$ , the capacitance remains at an almost constant value. When the potentials exceed  $0.5 \text{ V}$ , the capacitance again increases with potential. Similar behavior of capacitance-potential curves has also been

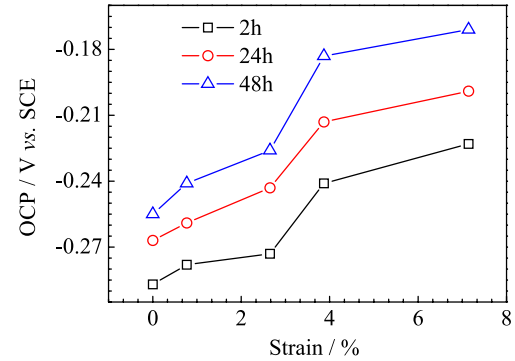


**Figure 5.** Evolution of OCPs for samples with different degree of deformation before the breakdown of passive films.

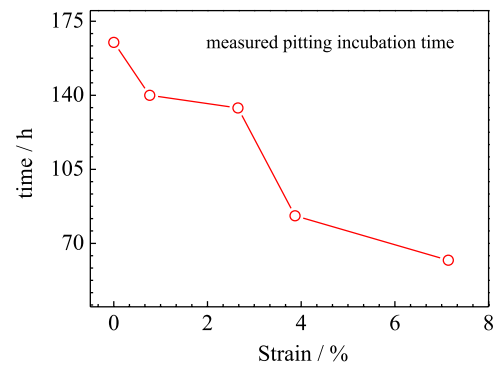


**Figure 6.** Pitting incubation time of samples with different degree of deformation in the cement extract.

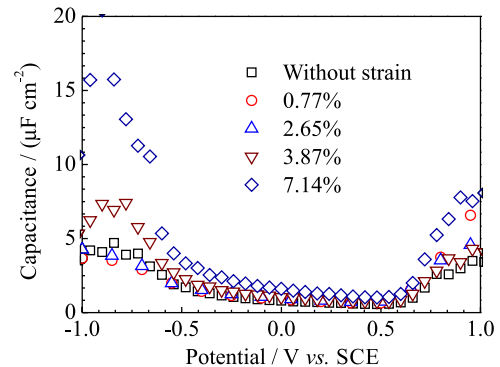


**Figure 7.** The capacitance-potential curves of samples with different degrees of deformation in cement extract after 2 h of passivation in pore solution at OCP.

observed by other authors.<sup>15,16</sup> In addition, it is clear that the capacitance increases with increasing plastic deformation in our study.

Figure 8 shows Mott-Schottky plots of samples with different degree of deformation after 2 h stabilization in the cement extract. In the range between  $-0.6$  and  $0.5 \text{ V}$ , two positive slopes and a break point at  $0 \text{ V}$  are observed. Schoonman *et al.*<sup>19</sup> attributed the non-linearity of Mott-Schottky plots to inhomogeneous donor distributions or surface roughness effects. The positive slopes suggest that the passive films on the carbon steel

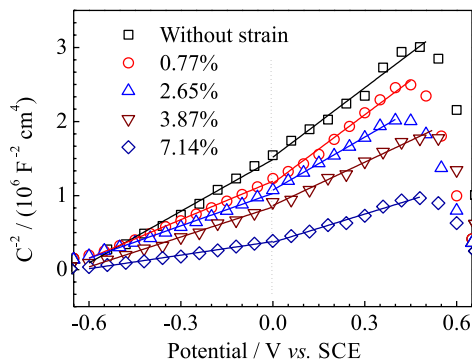


**Figure 8.** Mott-Schottky plots of the samples subjected to different degree of deformation in cement extract solution at the OCP for 2 h.

are n-type semiconductors.<sup>15,18,20</sup> In addition, according to equation (1),<sup>15,16</sup> the value of  $C^{-2}$  is closely related to the donor density ( $N_D$ ) of the passive films:

$$C^{-2} = \frac{2}{\epsilon\epsilon_0 q N_q} \left( E - E_{FB} - \frac{KT}{q} \right) \quad (1)$$

where  $\epsilon_0$  is the permittivity of free space ( $8.85 \times 10^{-14} \text{ F cm}^{-1}$ ),  $\epsilon$  is the dielectric constant of the passive film (15.6),<sup>15</sup>  $q$  is the electron charge ( $1.602 \times 10^{-19} \text{ C}$ ),  $k$  is the Boltzmann constant ( $1.38 \times 10^{-23} \text{ J K}^{-1}$ ), and  $N_D$  is the donor density of the passive film (which can be determined by the slope of the experimental  $C^{-2}$  versus  $E$  plots).  $E_{FB}$  is the flat band potential,  $T$  is the absolute temperature, and  $KT/q$  is negligible, as it is only about 25 mV at room temperature.<sup>18,20,21</sup>

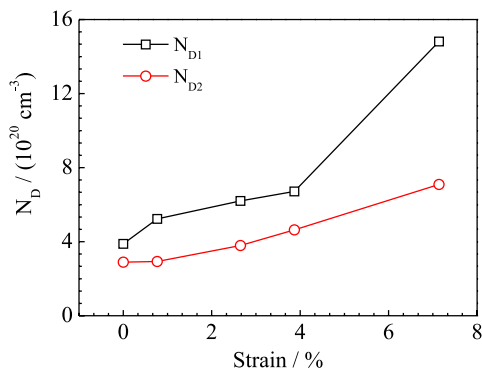


**Figure 9.** Evolutions of donor densities of passive films on the samples subjected to different strains in cement extract solution at the OCP for 2 h.

Marking a break point at 0 V (Figure 8), the donor density is defined as  $N_{D1}$  when the potential is below 0 V, and the donor density at potential higher than 0 V is defined as  $N_{D2}$ .  $N_{D1}$  and  $N_{D2}$  are deduced from the slopes of the Mott-Schottky plots and the results are presented in Figure 9. As the results show, the donor density is of the order of magnitude  $10^{20} \text{ cm}^{-3}$ . The same order of magnitude has been reported by Li *et al.*<sup>20</sup> for passive films

on carbon steel in a bicarbonate/carbonate buffer solution. In addition, in the present study, both donor density,  $N_{D1}$  and  $N_{D2}$ , clearly increased with increasing degree of deformation. According to the point defect model (PDM) proposed by Macdonald and co-workers,<sup>22-24</sup> the n-type donors in the passive film are mainly oxygen vacancies at the metal/film interface, and the high donor density (oxygen vacancies) means that there is a high probability for the aggressive anions ( $\text{Cl}^-$ ) to be absorbed in the surface oxygen vacancies. The anion-catalyzed cation vacancies are then concentrated on the metal/film interface at the regions with structural discontinuities.<sup>24</sup> The resulting cation vacancy condensation separates the films from the substrate and prevents further growth of the films. At the same time, the dissolution of passive films still takes place on the film/solution interface. Subsequently, rupture of passive films at the cation vacancy condensation region probably occurs. Consequently, a high donor density suggests that the passive film is susceptible to pitting corrosion.<sup>25</sup> In other words, the stability decreases with increasing donor density for n-type semiconducting passive films. The results presented in Figure 9, which are consistent with the polarization results (Figure 3) and OCP results (Figure 4), further confirm that serious deformation reduces the stability of the passive films.

On the other hand, as shown in Figure 9, the donor density  $N_{D1}$  is much higher than  $N_{D2}$ . This situation has been also reported by Li<sup>20</sup> and Hamadou.<sup>21</sup> It means that when the potential exceeds the break value in the Mott-Schottky plots, the donor density of passive films will be much lower than that below the break potential. Bojinov *et al.*<sup>26</sup> deduced that this phenomenon was closely related to the ionization of deep donors in the second donor level in the band gap. A previous study<sup>27</sup> has confirmed that the  $\text{Fe}_3\text{O}_4$  and  $\text{Fe}_2\text{O}_3$  in the passive film have an inverted spinel structure. This has 16 octahedral positions and 8 tetrahedral positions. The donors were formed by the substitution of  $\text{Fe}^{3+}$  ions by  $\text{Fe}^{2+}$  on the tetrahedral positions of  $\text{Fe}_2\text{O}_3$ .<sup>28</sup> When the potential exceeds the break potential (0 V),  $\text{Fe}^{2+}$  ions can be oxidized to  $\text{Fe}^{3+}$  ions, and the capacitance responses are controlled by the electronic structure of  $\text{Fe}_2\text{O}_3$  oxide in the passive film.<sup>20</sup> Subsequently, the second positive slopes are formed, so the donor density above the break potential ( $N_{D2}$ ) is lower than that below the break potential ( $N_{D1}$ ).

The thickness of the space charge layer ( $W$ ) at the passive film-electrolyte interface can be estimated from using equation (2).<sup>18,29,30</sup>

$$W = \left[ \frac{2\epsilon\epsilon_0}{qN_q} \left( E - E_{FB} - \frac{KT}{q} \right) \right]^{1/2} \quad (2)$$

The thicknesses of space charge layers for samples with different degree of deformation are presented in Figure 10. As the results show, the thicknesses are in the order of magnitude of nm and match the results reported by Simões *et al.*<sup>18</sup> Meanwhile, as the results from Okamoto *et al.*,<sup>30</sup> the thicknesses increase significantly as potential increases.

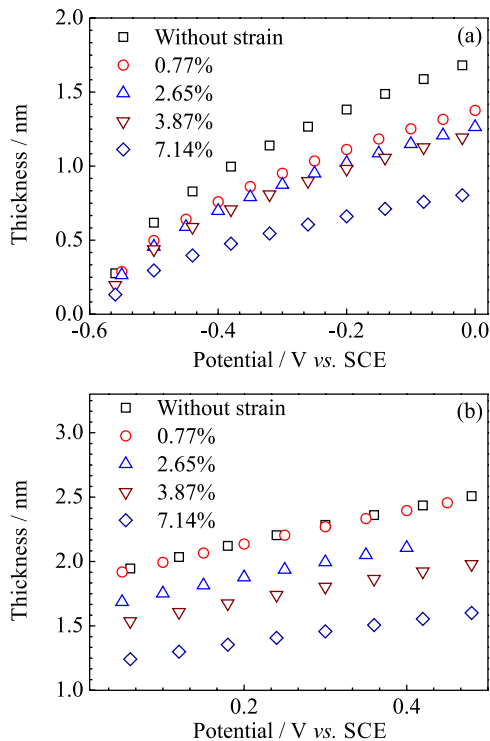


**Figure 10.** Thicknesses of space charge layers on carbon steel with different degree of deformation as a function of potential. (a) Thicknesses of space charge layers are below the break potential; (b) thicknesses of space charge layers exceed the break potential.

In addition, as shown in Figure 10, the thicknesses of space charge layers decrease with increasing plastic deformation. Interestingly, Sidane *et al.*<sup>9</sup> reported that the kinetic constant ( $k_0$ ) of the mediator oxidation on 304L stainless steel increases significantly as the tensile stress increased. The authors ascribed this situation to the acceleration of the rate of transport of the oxygen vacancies under stress. The results concerning space charge layers (Figure 10) in the present study support the conclusion from Sidane *et al.*<sup>9</sup> For the samples subjected to plastic deformation, space charge layers thinned as the deformation magnitude increased. In addition, the electrical field strength in the passive film is independent of the thickness and remains constant.<sup>12,17,22</sup> Thus, the thin space charge layer accelerates the rate of the transport of the oxygen vacancies in the passive film.<sup>21</sup> As a result, the kinetic constant ( $k_0$ ) of the mediator oxidation increases.

## AFM analysis of passive films

After 24 h of passivation in the pore solution, the passive films on carbon steels with different degree of deformation were investigated by AFM. Compared with the passive films (Figure 11) on control samples, the passive films on the heavily deformed samples (Figure 12) were much more uneven. On the other hand, when the samples were subjected to plastic deformation, the roughness of the substrate surface is also increased. Some researchers<sup>31-33</sup> studied the surface profiles of the substrate under plastic deformation using AFM, and the results confirmed that increasing numbers of slip bands or dislocation outcrops would increase the roughness of the substrate surface.

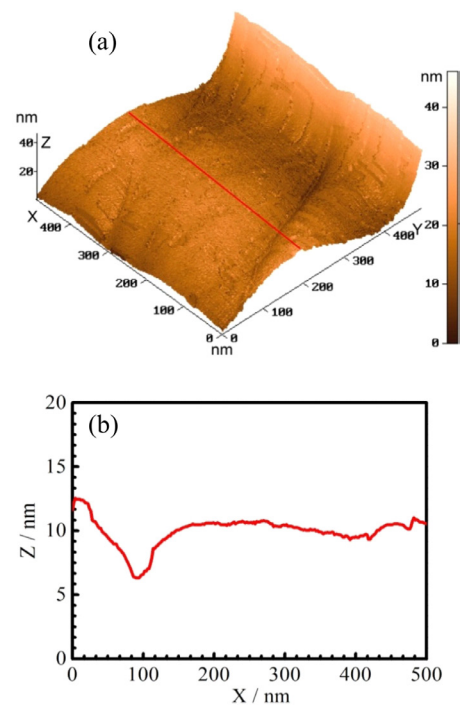


**Figure 11.** AFM micrographs of passive film on undeformed sample after immersion 24 h in cement extract. (a) 3D AFM micrographs; (b) surface profiles along the line depicted in Figure 11a.

According to the PDM,<sup>21-23</sup> the breakdown of a passive film may occur due to the anion-catalyzed cation vacancy condensation at structural discontinuities at the substrate/film interface, such as the outcrops of dislocations, slip bands, and second phase particles.<sup>23,31</sup> With increasing plastic deformation, the structural discontinuities on the surface will increase.<sup>31-33</sup> As a result, more anion-catalyzed cation vacancy condensation regions will form at the structural discontinuities, increasing the probability of passive film breakdown. Therefore, the AFM results, together with the polarization results (Figure 3) and

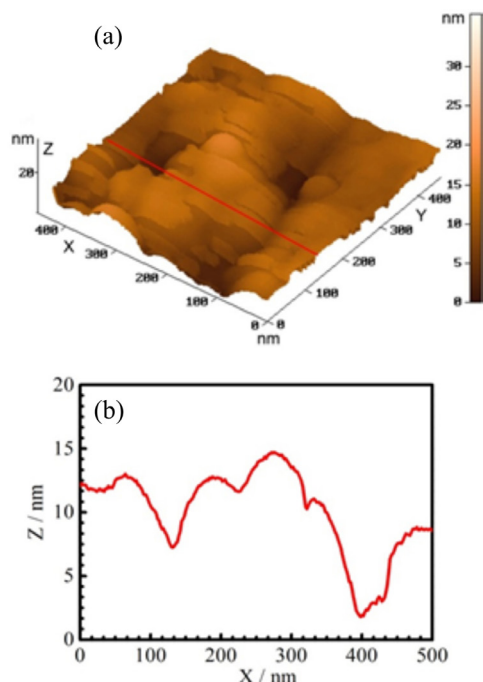


**Figure 12.** AFM micrographs of a passive film on the sample subjected to 7.14% plastic deformation after immersion 24 h in cement extract. (a) 3D AFM micrographs; (b) surface profiles along the line depicted in Figure 12a.

OCP results (Figure 4), support the conclusion that the stability of passive films decreases with increasing plastic deformation.

## Conclusions

In a cement extract solution, the OCP of carbon steel increases with increasing plastic deformation, while the pitting incubation time decreases as the plastic deformation increases. The current fluctuations occur frequently for samples experiencing high plastic deformation, suggesting that the serious deformation reduces the stability of the passive films. Moreover, the passive films on highly deformed carbon steel are heavily doped. The space charge layers are thinned as the magnitude of deformation increases. In addition, the high plastic deformation also accentuated the non-uniformity of the passive films. The high donor density and regions of structural discontinuities promoted condensation of anion-catalyzed cation vacancies on the films/substrate interface. Therefore, the stability of passive films on the deformed samples decreases with increasing plastic deformation.

## Acknowledgements

The authors would like to thank the National Natural Science Foundation of China (51301060, 51210001), the

Fundamental Research Funds for the Central Universities (2013B03514), and the Natural Science Foundation of Jiangsu Province (BK2011026) for support to this work.

## References

- Schroeder, R. M.; Müller, I. L.; *Corros. Sci.* **2003**, *45*, 1969.
- Vu, N. A.; Castel, A.; Francois, R.; *Corros. Sci.* **2009**, *51*, 1453.
- Yang, Q.; Luo, J. L.; *Electrochim. Acta.* **2001**, *46*, 851.
- Díaz, B.; Freire, L.; Nóvoa, X. R.; Pérez, M. C.; *Electrochim. Acta.* **2009**, *54*, 5190.
- Vignal, V.; Oltra, R.; Verneaub, M.; Coudreuse, L.; *Mater. Sci. Eng. A.* **2001**, *303*, 173.
- Vignal, V.; Valot, C.; Oltra, R.; Verneau, M.; Coudreuse, L.; *Corros. Sci.* **2002**, *44*, 1477.
- Zhang, G. A.; Cheng, Y. F.; *Corros. Sci.* **2010**, *52*, 960.
- Vignal, V.; Delrue, O.; Heintz, O.; Peultier, J.; *Electrochim. Acta.* **2010**, *55*, 7118.
- Sidane, D.; Devos, O.; Puiggali, M.; Touzet, M.; Tribollet, B.; Vivier, V.; *Electrochim. Commun.* **2011**, *13*, 1361.
- Zhu, R. K.; Luo, J. L.; *Electrochim. Soc.* **2010**, *12*, 1752.
- Ghods, P.; Isgor, O. B.; Meraeb, G.; Miller, T.; *Cem. Concr. Compos.* **2009**, *31*, 2.
- Carnot, A.; Frateur, I.; Zanna, S.; Tribollet, B.; *Corros. Sci.* **2003**, *45*, 2513.
- Lee, C. T.; Qin, Z.; Odziemkowski, M.; Shoesmith, D. W.; *Electrochim. Acta.* **2006**, *51*, 1558.
- Farmer, J. C.; Haslam, J. J.; Day, S. D.; *FY05 HPCRMA Annual Report: High-Performance Corrosion-Resistant Iron-Based Amorphous Metal Coatings Evaluation of Corrosion Reistance FY05 HPCRMA Annual Report #Rev. IDOEDARPA Co-Sponsored Advanced Materials Program, UCRL-TR-234799*, 2007.
- Cheng, Y. F.; Luo, J. L.; *Electrochim. Acta.* **1999**, *44*, 2947.
- Dong, Z. H.; Shi, W.; Zhang, G. A.; Guo, X. P.; *Electrochim. Acta.* **2011**, *56*, 5890.
- Joiret, S.; Keddad, M.; Novoa, X. R.; Perez, M. C.; Rangel, C.; Takenouti, H.; *Cem. Concr. Compos.* **2002**, *24*, 7.
- Simões, A. M. P.; Ferreira, M. G. S.; Rondot, B.; Belo, M. C.; *J. Electrochem. Soc.* **1990**, *137*, 82.
- Schoonman, J.; Vos, K.; Blasse, G.; *J. Electrochem. Soc.* **1981**, *128*, 1154.
- Li, D. G.; Feng, Y. R.; Bai, Z. Q.; Zhu, J. W.; Zheng, M. S.; *Electrochim. Acta.* **2007**, *52*, 7877.
- Hamadou, L.; Kadri, A.; Benbrahim, N.; *Appl. Surf. Sci.* **2005**, *252*, 1510.
- Chao, C. Y.; Lin, L. F.; Macdonald, D. D.; *J. Electrochem. Soc.* **1981**, *128*, 1187.
- Macdonald, D. D.; *J. Electrochem. Soc.* **1992**, *139*, 3434.
- Macdonald, D. D.; *Pure. Appl. Chem.* **1999**, *71*, 951.

25. Cheng, Y. F.; Luo, J. L.; *Appl. Surf. Sci.* **2000**, *167*, 113.
26. Bojinov, M.; Fabricius, G.; Laitinen, T.; Makela, K.; Saario, T.; Sundholm, G.; *Electrochim. Acta.* **2000**, *45*, 2029.
27. Kuroda, K.; *J. Electrochem. Soc.* **1982**, *129*, 2163.
28. Hakiki, N. E.; Cunha, B. M. D.; Simoes, A. M. P.; *J. Electrochem. Soc.* **1998**, *145*, 3821.
29. König, U.;Schultze, J. W.; *Solid State Ionics*, **1992**, *53-56*, 255.
30. Okamoto, G.; *Corros. Sci.* **1973**, *13*, 471.
31. Chandrasekaran, D.; Nygåards, M.; *Mater. Sci. Eng. A.* **2004**, *365*, 191.
32. Wejdemann, C.; Pedersen, O. B.; *Mater. Sci. Eng. A.* **2004**, *387-389*, 556.
33. Polák, J.; Petrevec, M.; Man, J.; *Mater. Sci. Eng. A.* **2005**, *400-401*, 405.

Submitted: September 22, 2013

Published online: January 10, 2014